Release of alkali salts and coal volatiles affecting internal components in fluidized bed combustion systems

E. Arias del Campo*, A. Keer-Rendon*, L. Manzanares-Papayanopoulos* and R. Bautista-Margulis**

Abstract

In spite of the potential advantages of atmospheric fluidized bed systems, experience has proved that, under certain environments and operating conditions, a given material employed for internal components could lead to catastrophic events. In this study, an attempt is made to establish material selection and operational criteria that optimize performance and availability based on theoretical considerations of the bed hydrodynamics, thermodynamics and combustion process. The theoretical results may indicate that, for high-volatile coals with particle diameters (d_c) of 1-3 mm and sand particle size (d_s) of 0.674 mm, a considerable proportion of alkali chlorides may be transferred into the freeboard region of fluidized bed combustors as vapor phase, at bed temperatures (T_b) < 840 °C, excess air (XSA) ≤ 20 %, static bed height (H_s) ≤ 0.2 m and fluidizing velocity (U_o) < 1 m/s. Under these operating conditions, a high alkali deposition may be expected to occur in heat exchange tubes located above the bed. Conversely, when the combustors operate at T_b > 890 °C and XSA > 30 %, a high oxidation rate of the in-bed tubes may be present. Nevertheless, for these higher T_b values and XSA < 10 %, corrosion attack of metallic components, via sulfidation, would occur since the excessive gas-phase combustion within the bed induced a local oxygen depletion.

Keywords Alkali deposition. Oxidation-sulfidation mechanism. Combustion modeling. Devolatilization kinetics. Fluidized beds.

Liberación de sales alcalinas y volátiles del carbón que afectan componentes internos en sistemas de combustión de lecho fluidizado

Resumen

A pesar de las ventajas potenciales de los sistemas atmosféricos de lecho fluidizado, la experiencia ha demostrado que, bajo ciertas atmósferas y condiciones de operación, un material que se emplea como componente interno podría experimentar una falla y conducir a eventos catastróficos. En este estudio, se intenta establecer un criterio tanto operativo como de selección del material que permita optimizar su disponibilidad y funcionalidad basados en consideraciones teóricas de la hidrodinámica del lecho, la termodinámica y el proceso de combustión. Los resultados teóricos indican que, para carbones de alto contenido de volátiles con diámetros de partícula (d_c) de 1-3 mm y tamaños de partícula de arena (d_s) de 0,674 mm, una cantidad considerable de cloruros alcalinos podrían ser transferidos como fase vapor en la región del espacio libre de los combustores de lecho fluidizado a temperaturas de lecho (T_b) < 840 °C, excesos de aire (XSA) ≤ 20 %, alturas estáticas de lecho (H_s) ≤ 0,2 m y velocidades de fluidización (U_o) < 1 m/s. Bajo estas condiciones de operación, se espera que ocurra una alta deposición alcalina en los tubos de intercambio de calor localizados arriba del lecho. Por el contrario, cuando los combustores operan a T_b > 890 °C y XSA > 30 %, es probable que se presenten altas velocidades de oxidación de los tubos inmersos en el lecho. No obstante, a estas altas T_b y XSA < 10 %, ocurriría un ataque de corrosión (vía sulfidación) de los componentes metálicos ya que, presumiblemente, la combustión excesiva de fase-gas dentro del lecho induciría a un agotamiento local del oxígeno.

Palabras clave Deposición alcalina. Mecanismo de oxidación-sulfidación. Modelación de la combustión. Cinética de devolatilización. Lechos fluidizados.

(*) Centro de Investigación en Materiales Avanzados, S.C. (CIMAV), División de Deterioro de Materiales, Miguel de Cervantes 120, Complejo Industrial Chihuahua, C.P. 31109, Chihuahua-Chihuahua, México.

(**) Universidad Juárez Autónoma de Tabasco (UJAT), División Académica de Ciencias Biológicas, Carretera Villahermosa-Cárdenas Km. 0.5, C.P. 86090, Villahermosa-Tabasco, México.

1. INTRODUCTION

Industrial power plants utilizing fluidized bed combustors (FBC) have been developed and operated worldwide. This type of combustion systems are known to have a number of advantages over the more conventional combustion techniques, among them: *i)* large reduction of sulfur oxides (SOx) can be attained by adding limestone or dolomite to the bed, *ii)* lower formation of nitrogen oxides (NOx) are encountered because of their typical operating temperatures (850 °C), *iii)* heat transfer rates for the equivalent combustor area/volume ratio are higher due to the addition of conduction heat transfer from the bed particles to the boiler tubes and walls, and *iv)* the ability to burn low grade fuels and waste materials with high combustion efficiencies (85-99 %). In practice, however, all combustion systems experience materials problems and there are a number of critical components whose durability may limit the system performance.

From the above mentioned advantages, the low combustion temperature suggested to early investigators that the release of corrosive materials (i.e. alkali metal salts, vanadium pentoxide, etc.) would be greatly reduced compared to conventional combustion systems, and that sintered deposits would be unlikely to build up on the heat exchange surface. As a result, the fireside corrosion of the hot metal components was expected to be minimal. In addition no ash melting or sintering was expected to occur, and combining these aspects with the relatively low gas velocities, erosion would then be a minor problem. Nevertheless, experience has proved otherwise[1 and 2].

In this context, a number of studies[3 and 4] have reported that the occurrence of undesirable high temperatures (up to 200-300 °C in excess of the bed temperature) due to the volatiles combustion which escaped unburnt from the bed has led to serious problems in prototypes and commercial installations of such FBC systems (i.e. damage of materials of construction due to hot spots, fouling and corrosion of the heat transfer surfaces by softened ash, high CO and NO_x emission levels, etc.). Likewise, salts of alkali metals may worsen deposition by cementing deposited particles[5 and 6], and may accelerate hot corrosion, especially by combined action with other species such as sulfur trioxide. Hence the formation of chlorides, which arise from the chlorine content in the coal, may be troublesome[7 and 8]. Low oxygen activity in FBC fuel beds can also lead to new problems because the usual protective oxide films may not develop on metal surfaces, and alternating reducing and oxidizing conditions bring up a wholly new environment for heat-receiving tube banks[9].

In the present investigation, an attempt is made to determine the fraction of fuel burnt as volatiles in the bed region by modeling their evolution and combustion within the bed. From this theoretical framework, a thermochemical approach may then be incorporated to the present model to provide new basic information on the occurrence of both volatilized alkali metals and sulfidation/oxidation mechanisms. Therefore, the extent of external corrosion on heat transfer surfaces in the FBC may be predicted under various operating and fluidizing conditions.

2. MODELING APPROACH

2.1. Thermodynamic equilibrium of alkali salts

In any analysis of deposition and corrosion processes, it is essential to know whether the alkali salts are present as vapor or predominantly as a condensed phase: liquid or solid. The saturation vapor pressures and possible reactions of the components involved must therefore be considered. Reactions of alkali compounds with sulfur trioxide may form alkali sulfates which could condense out to remove the alkalis from the vapor phase. In addition to this sulfate condensation, serious problems occur under reducing conditions when sulfides are present[8]. The specific reactions may be given as,

$$SO_{2(g)} + 1/2\ O_{2(g)} \Leftrightarrow SO_{3(g)} \quad (1)$$

$$2NaCl(g) + H_2O_{(g)} + SO_{2(g)} + 1/2\ O_{2(g)} \Leftrightarrow Na_2SO_{4(c)} + 2\ HCl_{(g)} \quad (2)$$

$$2\ KCl(g) + H_2O_{(g)} + SO_{2(g)} + 1/2\ O_{2(g)} \Leftrightarrow K_2SO_{4(c)} + 2HCl_{(g)} \quad (3)$$

The equilibrium constants for these reactions can be estimated from the JANAF tables and other thermochemical data which, in turn, can be surveyed in the literature[10 and 11]. Under typical FBC conditions, it may be assumed that sulfur is present in gases only as sulfur dioxide[12 and 13].

2.2. Modeling of gas-phase combustion

The present model was produced by comparing experimental data obtained in a calorimetric FBC

with various mathematical models for the combustion of coal volatiles in these systems. In accordance with previous investigations[14 and 15], the current modeling was divided into three basic stages: 1) bed hydrodynamics, 2) devolatilization kinetics and 3) oxygen requirements for combustion. The numerical scheme for solving the mathematical expressions in the model is shown in figure 1. For conceptual and mathematical convenience, the following assumptions have been made:

- the heat of reaction for volatiles decomposition and the latent heat of forming water vapor are neglected;
- the rate of heat loss from the coal particle is greater than the heat generation rate;
- the temperature within a particle is uniform, due to its small Biot number and low moisture content;
- as volatiles are released from a coal particle during thermal decomposition, the density of the remaining char decreases without any change in particle diameter;
- the combustion of volatiles is controlled by the mixing of the gaseous volatiles and oxygen in the bed;
- the evolution of each product is governed by a first-order process with a rate constant, k, which varies with volatile species but is independent of coal type.

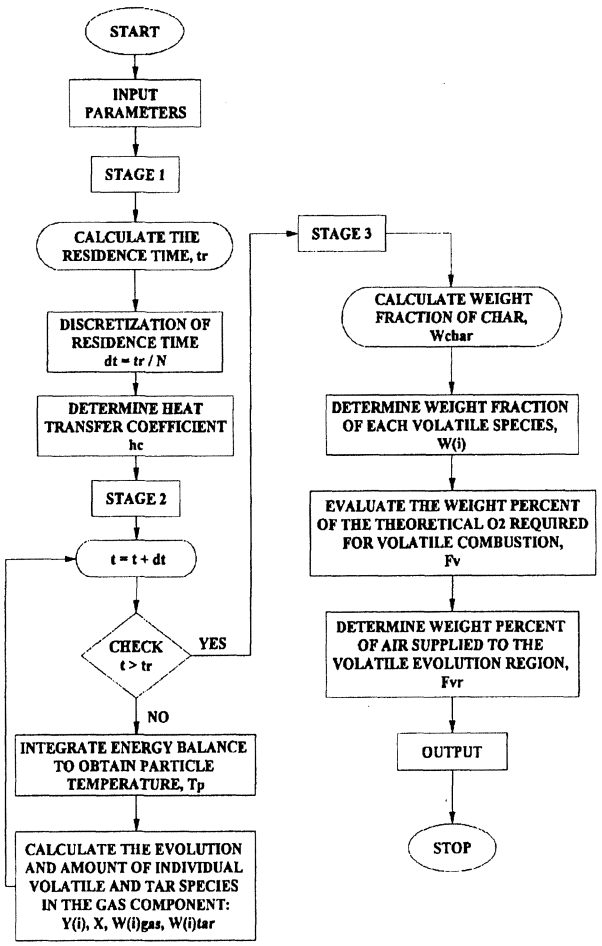

Figure 1. Algorithm for solving the model.

Figura 1. Algoritmo para resolver el modelo.

The calculation of the bed hydrodynamics is carried out to obtain the residence time of a coal particle, τ_r, reaching the bed surface as follows:

$$\tau_r = \frac{H_{max}}{U_r} \tag{4}$$

where the mean axial velocity for the particle, U_r, is given by[16]

$$U_r = 0.15\ (U_o - U_{mf})^{0.5} \tag{5}$$

and the maximum bed height, H_{max}, may be obtained from

$$H_{max} = \left[1 + \left(\frac{U_o - U_{mf}}{U_b}\right)\right] H_{mf} \tag{6}$$

where U_o is the superficial velocity, U_b is the absolute bubble rise velocity, U_{mf} is the minimum fluidizing velocity and H_{mf} is the bed height at minimum fluidizing velocity.

From the residence time of the coal particle (τ_r) and the radial dispersion coefficient (D_r), the mean radial displacement of the coal particle, R_V, can be determined from the two-dimensional Einstein diffusion equation as:

$$R_V = (4\ D_r\ \tau_r)^{0.5} \tag{7}$$

The total heat transfer coefficient to the particle, h_c, is calculated from the summation of the respective particle-to-particle[17], h_{pp}, and gas-to-particle[18], h_{gp}, heat transfer contributions. Hence h_{pp} can be evaluated from:

$$h_{pp} = 25.06\ \rho_c^{0.2}\ k_g^{0.6}\ d_c^{-0.36} \tag{8}$$

where k_g is the thermal conductivity of the gas surrounding the coal particle, ρ_c is the density of the coal particle, d_c is the coal diameter, and:

$$h_{g\,p} = 0.095\ \mathrm{Re}^{-0.12}\ Cp_g\ \rho_g\ U_0 \qquad (9)$$

where *Re* is the Reynolds number and Cp_g is the specific heat of the gas, so that:

$$h_c = h_{pp} + h_{gp} \qquad (10)$$

The temperature increase of the coal particle is computed by numerical integration of the energy balance which accounts for both radiative and convective heat transfer, by using a fourth-order Runge-Kutta scheme. The balance takes the form:

$$m_p\ Cp_c \left(\frac{dT_p}{dt}\right) = A_p\left[\sigma\ \varepsilon\left(T_b^4 - T_p^4\right) + h_c\left(T_b - T_p\right)\right] \qquad (11)$$

where *Ap* is the constant surface area of the particle, m_p is the mass of the particle, Cp_c is the specific heat capacity of the coal, T_p is the particle temperature, T_b is the bed temperature, ε is the emissivity of the coal particle and σ is the Stefan-Boltzman constant.

From the devolatilization kinetics standpoint, a previous modeling approach[19] has been used because it is capable of yielding the evolution rate for each volatile species and tar. In this kinetic approach, the coal is represented as an area with *X*- and Y-dimensions for modeling the two paths during thermal decomposition. Y_i^o represents the initial mass fraction of a particular component (e.g. carboxyl, aromatic hydrogen) and the sum of all Y_i^o is 1. Hence the evolution of each gas component is represented by first-order diminishing of the Y_i dimension :

$$Y_i = Y_i^o\ \exp\ (-k_i\ t) \qquad (12)$$

The volatiles evolution is initially divided into potential tar-forming (X^o) and a non-tar-forming ($1 - X^o$) fractions, and is subsequently represented by first-order diminishing of the tar-forming *X*-domain,

$$X = X^o\ \exp\ (-k_x\ t) \qquad (13)$$

The mass fraction W_{char} of the original particle that remains as char may be calculated from the *X*- and Y-dimension values at any time as:

$$W_{char} = \sum_{i=1}^{9}(1 - X^o)\,Y_i + \sum_{i=1}^{9} XY_i = \left(1 - X^o + X\right)\sum_{i=1}^{9} Y_i \qquad (14)$$

and the particle mass in equation (11) may then be related to its initial value as:

$$m_p = m_p^o\ W_{char} \qquad (15)$$

The rate constants used in the model are listed in table I. In the absence of volatile analyses for the coals modeled here, the values of the coal parameters were taken as those given by Lee *et al.*[14] for a high-volatile Montana lignite (i.e. $Y^\circ_{\ 1} = 0.10$, $Y^\circ_{\ 2} = 0.032$, $Y^\circ_{\ 3} = 0.060$, $Y^\circ_{\ 4} = 0.156$, $Y^\circ_{\ 5+6} = 0.0106$, $Y^\circ_{\ 7} = 0.11$, $Y^\circ_{8} = 0.018$, and $X^\circ = 0.11$).

The weight percent F_V of the in-bed volatiles combustion (at stoichiometric conditions) is estimated by computing the ratio of the theoretical oxygen required for the combustion of 1 g of volatiles, which is evaluated from the mass fraction, W_i, of each volatile species remaining in the char (calculated as the ratio of Y_i and the sum of the Y_i), and the theoretical oxygen requirement for the combustion of 1 g of the parent coal :

$$F_V = \frac{16(W_{CO}/28) + 16(W_{NV}/14) + 32(W_{HV}/4) + 46.4(W_{CH1.8}/13.8) + W_{SV}}{32(W_C/12) + 32(W_H/4) + 16(W_N/14) + W_s - W_o} \qquad (16)$$

The weight percent, F_{VR}, of air supplied to the volatiles release zone may be determined from the ratio of the areas of the volatiles evolution region and the horizontal cross-section of the bed (approximated by a circle of radius 0.1 m centered on the injector), as:

$$F_{VR} = (100 + XSA)\left(\frac{R_V}{0.1}\right)^2 \qquad (17)$$

where *X*SA is the percentage excess air.

Finally, the fraction, F_{VRB}, of the volatile material released and burnt in the bed region can be deduced from:

Table I. Kinetic constants used in the present mode[14]

Tabla I. Constantes cinéticas usadas en el presente modelo[14]

Functional group of product	Kinetic rates (s^{-1})
Carboxyl	$k_1 = 75\ \exp\ (-5800 / T_p)$
Hydroxyl	$k_2 = 370\ \exp\ (-6900 / T_p)$
Ether loose	$k_3 = 87000\ \exp\ (-12000 / T_p)$
Ether tight	$k_4 = 4 \times 10^9\ \exp\ (-35000 / T_p)$
Nitrogen loose	$k_5 = 200\ \exp\ (-7600 / T_p)$
Nitrogen tight	$k_6 = 290\ \exp\ (-12700 / T_p)$
Light hydrocarbons	$k_7 = 33000\ \exp\ (-12000 / T_p)$
Aromatic hydrogen	$k_8 = 3600\ \exp\ (-12700 / T_p)$
Non-volatile carbon	$k_9 = 0$
Tar and heavy hydrocarbons	$k_x = 9300\ \exp\ (-9800 / T_p)$

$$F_{VRFB} = \left(\frac{F_{VR}}{F_V} \right) \quad (18)$$

3. EXPERIMENTAL

The experimental work was carried out in a 0.2 m internal diameter mild steel combustor which was designed in a calorimetric mode. Ignition of the bed was attained via a special propane-delivery device attached to a distributor plate of the "standpipe type". The coal feeding system was underbed and pneumatic, having a coal particle size distribution between 0.71 and 4.75 mm. The bed material was made up of silica sand with an average particle size of 0.674 mm. and a static bed height of 0.2 m. Limestone was not added to the sand bed. Table II shows the chemical analysis of the coals employed in this work. The operating and fluidizing ranges used in the calorimetric combustor are summarized in table III.

Based on calorimetric principles, energy and material balances were performed on the bed region which was taken as the control volume. The conservation equations accounted for: a) the total heat released in the bed, Q_b ; b) the total heat released in the freeboard, Q_{fb} ; c) the heat losses in the solid and gas streams, Q_{lsg} ; and d) the heat losses to surroundings, Q_{ls} [20], as shown in figure 2.

Table II. Chemical analysis of the fuels used in the experiments

Tabla II. Análisis químicos de los combustibles usados en los experimentos

COAL TYPE	CLIPSTONE-1 (C / E - 1)	CALVERTON-1 (CALV -1)	CLIPSTONE-2 (C / E - 2)
Proximate Analysis (wt% air-dried):			
Fixed Carbon	54.9	53.4	53.9
Volatile Matter	33.7	36.6	31.1
Ash	10.0	5.1	12.0
Moisture	1.4	4.9	3.0
Ultimate Analysis (wt% air-dried):			
Carbon	68.4	72.9	70.3
Hydrogen	5.2	5.1	5.1
Nitrogen	1.4	1.3	0.9
Sulfur	1.7	1.1	2.0
Water	1.4	4.9	3.0
Oxygen	11.8	9.6	6.7
Ash	10.0	5.1	12.0
Higher Heating Value (kJ/kg)	30 492	29 809	28 957

Table III. Operating and fluidizing conditions setup for the experimental runs

Tabla III. Condiciones de operación y fluidización establecidas para las corridas experimentales

Variable	Value(s)	Units
Bed temperature, T_b	800 - 900	°C
Excess air, *XSA*	7 - 41	%
Coal diameter, d_c †	0.71 - 4.75	mm
Sand diameter, d_s	0.674	mm
Static bed height, H_s	0.20	m
Superficial velocity, U_o	0.52 - 1.35	m/s
Coal mass flowrate, F_c	2.10 - 3.95	kg/h

† One size level with a size distribution between 0.71 and 4.75 mm.

In addition, the total heat released in the bed comprised an individual measurement and/or calculation of : 1) the heat given off from gases, Q_g; 2) the sensible heat from carbon in the bed, Q_{cb}; 3) the heat removed by cooling probes, Q_w; and 4) the heat radiated back to the bed, Q_r [21]. The heat losses in solid and gas streams were estimated from: 1) the heat released by carbon as sensible heat in the exit flue gases, Q_{shc} ; 2) the heat lost when carbon is burned to CO instead of CO_2, Q_{co} ; 3) the unburnt carbon carryover, Q_{uc} ; and 4) the enthalpy of water vapor in the combustion gases, Q_{wv2} [22]. Therefore the energy fraction of the volatile component (∇_{vf}) transferred into the freeboard and burnt there was deduced as a degree of freedom from the overall energy balance, as follows:

$$\nabla_{vf} = \left(\frac{\dot{Q}_{vf}}{\dot{Q}_t + \dot{Q}_{wv1}} \right) \quad (19)$$

where,

$$\dot{Q}_{vf} = (\dot{Q}_t + \dot{Q}_{wv_1}) - (\dot{Q}_g + \dot{Q}_{cb} + \dot{Q}_w + \dot{Q}_r) - \\ - (\dot{Q}_{shc} + \dot{Q}_{co} + \dot{Q}_{uc} + \dot{Q}_{cfb} + \dot{Q}_{wv_2}) - \dot{Q}_{ls} \quad (20)$$

and

$$\dot{Q}_t = F_c \, HHV_c \quad (21)$$

The total heat input, Q_t, was accurately determined from the coal mass flow rate supplied to

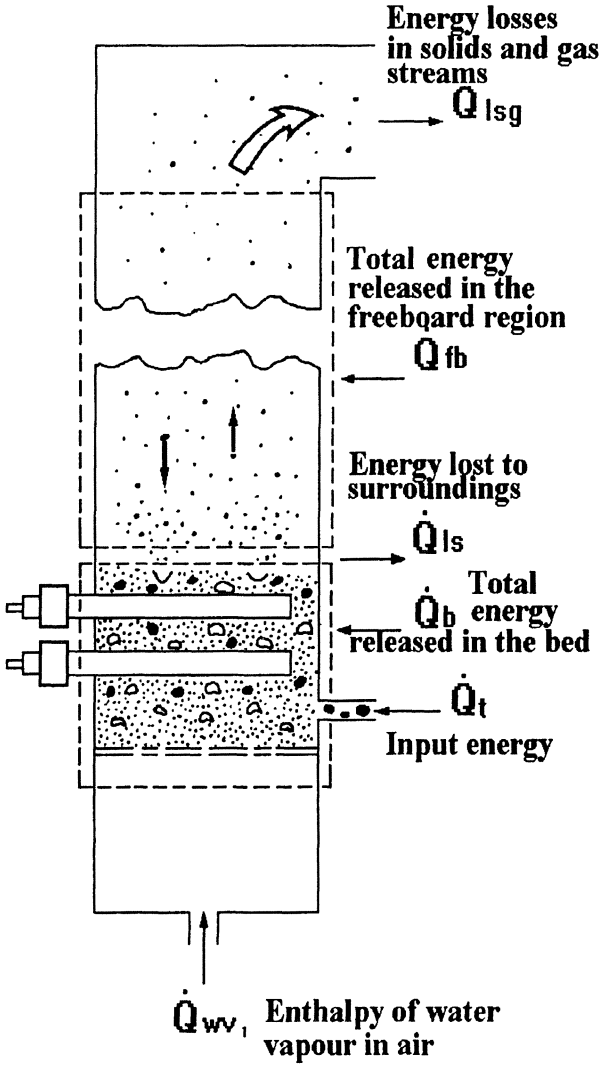

Figure 2. Heat flow diagram of the combustor.

Figura 2. Diagrama de flujo de calor del combustor.

the bed, F_c, and the higher heating value of the coal, HHV_c, adding the enthalpy of water vapor in the incoming air, Q_{wv1}[22]. Therefore the volatile fraction released and burnt in the bed (∇_{vb}) was obtained as

$$\nabla_{vb} = 1 - \nabla_{vf} \qquad (22)$$

4. RESULTS AND DISCUSSION

4.1. Combustion of coal volatiles in a FBC

Figure 3 shows both the theoretical calculation and the experimental measurements of the fraction of fuel burnt in the bed by the volatile component as a function of the *XSA* level at various bed temperatures. The actual modeling approach

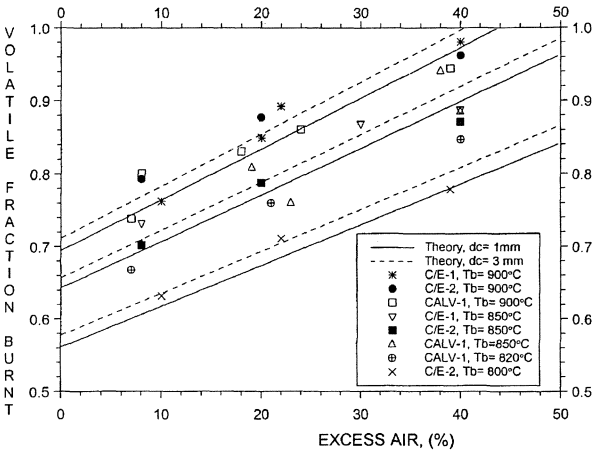

Figure 3. Influence of excess air on the combustion of coal volatiles in the bed region: Tb= 800-900 °C, d_s= 0.674 mm, H_s= 0.2 mm, U_{mf}= 0.32 m/s.

Figura 3. Influencia del exceso de aire sobre la combustión de volátiles de carbón en la región del lecho: Tb= 800-900 °C, d_s= 0.674 mm, H_s= 0.2 mm, U_{mf}= 0.32 m/s

indicates that the fraction of volatiles combusted in the hot bed is influenced by the mean radial dispersion coefficient, D_r, of the coal particle (see Eqs. 7 and 17). For each operating condition, a given value of D_r was inferred to give the best fit to the experimental data. The inferred values of D_r ranged, for the three coals examined, from 1.122 $\times$ 10^{-4} to 5.828 $\times$ 10^{-3} m^2/s at T_b = 800-900 °C, *XSA* = 10-40 %, d_c = 1-3 mm, d_s = 0.674 mm and H_s = 0.2 m. Under these operating and fluidizing conditions, the extent of volatiles combustion in the bed region was computed to be between 61.11 and 99.91 %.

Fundamentally viewed, the coal volatiles are likely to be spatially released and burnt within the bed (as an evolution region) due to solid dispersion which, in turn, will be influenced by bubble growth. At this point, it is worth mentioning that the bubble formation was specifically correlated in the model calculations to match the present experimental distributor design of the "standpipe" type. In spite of the consistency of the theoretical and experimental data obtained here, conclusions with regard to the D_r values used in this investigation, when scaling-up to commercial units, should be drawn with caution. From the above theoretical assessment, the bubble to particulate phase mass transfer played an important role on the in-bed volatiles combustion.

On the other hand, the assumptions regarding the isothermal behaviour of the coal particle sizes modeled in this work as well as the decrease in

particle density without significant shrinkage, described well the mechanistic pattern that coal volatiles undergo during pyrolysis in a hot sand bed. Further, the current kinetic approach applied in the model calculations, may be a good indication that the pyrolysis products were formed through multiple independent reactions. Hence it is suggested that the devolatilization process of such particle sizes, under typical FBC conditions, is likely to be kinetically controlled and that small Biot numbers (B_i=0.1-2) should be used for modeling volatiles combustion in FBC systems when a considerable proportion of the feed has a d_c < 3 mm. As expected, the evolution and burning of the volatile material within the bed have also been shown to be fairly sensitive to particle temperature according to the numerical solution applied in equation (11). Presumably both convective (external resistance) and intraparticle (internal resistance) heat transfer of the coal particle were important, affecting the volatile release rate.

4.2. Behaviour of alkali compounds in a FBC

Figure 4 shows the predicted equilibrium conversion of alkali chlorides to sulfates for the flue gas composition given in table IV. From this illustration, up to 32 % of the potassium is predicted to remain as vapor chloride at T_b = 900 °C; while 11 and 3 % of the potassium should remain in the vapor phase as chloride at T_b = 850 and 800 °C respectively. For sodium, a lower

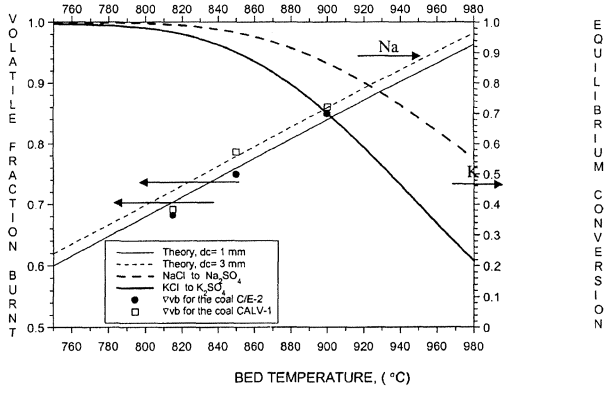

Figure 4. Effect of bed temperature on both the combustion of coal volatiles and the conversion of alkali chlorides to sulfates in the bed region: XSA= 20 %, d_s= 0.674 mm, H_s= 0.2 mm, U_{mf}= 0.32 m/s.

Figura 4. Efecto de la temperatura del lecho sobre la combustión de volátiles de carbón y la conversión de clorudos alcalinos a sulfatos en la región del lecho: XSA= 20 %, d_s= 0.674 mm, H_s= 0.2 mm, U_{mf}= 0.32 m/s.

Table IV. Flue gas composition for a specific theoretical calculation

Tabla IV. Comparación del flujo de gas para un cálculo teórico específico

GAS MEASURED	CONCENTRATION
O_2	3.2 %
CO_2	15.1 %
SO_2	420 ppm
H_2O	4.3 %
N_2	Balance

equilibrium conversion is predicted with the current theoretical calculation. Thus, maximum values of 3 and 13 % of sodium may be present as vapor chloride for the corresponding T_b = 850 and 900 °C. However, sodium chloride apparently remains in the vapor phase with values less than 1 % for $T_b \leq$ 830 °C. These estimates are sensitive to gas composition, meaning that small traces of hydrogen chloride will displace the equilibrium in reactions (1) and (2) to the left. Therefore, the proportion of alkali chloride in the vapor phase will be increased.

For shallow beds at T_b < 840 °C and *XSA* ≤ 20 %, over one fourth of the volatile matter may be transferred and burnt in the freeboard region. Under these operating conditions, the coal volatiles released above the bed are likely to be accompanied by an important proportion of alkali chloride in the vapor phase, as described earlier. Also, an increase in gas temperature in this region (due to excessive volatiles combustion) would certainly affect the extent of corrosion in the hotter parts of the ash deposit which then migrates towards the metal surface. From these results, a low alloy steel, say T-22, subjected to a maximum metal surface temperature of 600 °C, may be suitable for heat exchange tubes in the freeboard region[2].

On the other hand, at Tb > 890 °C and XSA > 30 %, accelerated oxidation of in-bed tubes may be induced since a good proportion of the alkali sulfates are expected to be present predominantly as a condensed phase (see Fig. 4). However, accurate information has not been found for the various contributions leading to this mechanism of fireside corrosion, namely: mechanical disruption of the protective oxide by erosion; dissolution of the oxide by the salt; or transport of sulfur through the oxide. Likewise, at higher Tb and XSA < 10 %, internal sulfidation of the tubes may rapidly take place giving rise to hot corrosion problems. As

expected, reducing conditions would promote low local oxygen activity so that high sulfur partial pressures may be generated. Clearly, local reducing environments are likely to be formed when oxygen is entirely consumed during the combustion of volatile matter within the bed. The selection of coals with low volatile alkali content would certainly help to diminish this pattern of corrosion attack. These preliminary data may suggest that a Type 347H austenitic stainless steel, having a maximun metal surface temperature of 760 °C, would be the best candidate for in-bed tube materials in FBC[2 and 13]. Although the use of these high alloy steels means higher costs, the compromise has to be made, especially when the coals present high chlorine contents. Notwithstanding the encouraging results obtained in this investigation, it is recommended that further experimental work should be conducted to parametrically confirm the previous statement.

5. CONCLUSIONS

The modeling of the bed hydrodynamics and the kinetics of devolatilization, coupled with a calculation of the theoretical oxygen required for the volatiles within an evolution region in the bed, has satisfactorily predicted the combustion of coal volatiles for a fluidized bed combustor. For high-volatile coals with d_c < 5 mm, the evolution of volatiles in the bed is mechanistically controlled by both diffusion and chemical kinetics, while the mixing process of volatiles and oxygen in the bed region is the determining step for the gas-phase combustion.

For the fluidizing conditions set up in this investigation, a considerable proportion of alkali chlorides may be transferred into the freeboard region of such systems as a vapor phase, for T_b < 840 °C and $XSA \leq 20$ %. Under these operating conditions, a high alkali deposition may be expected to occur in heat exchange tubes located above the bed. Conversely, when the FBC operates at T_b > 890 °C and XSA > 30 %, a high oxidation rate of the in-bed tubes may occur. Nevertheless, for these higher T_b values and XSA < 10 %, corrosion attack of metallic components, via sulfidation, would probably occur since the excessive gas-phase combustion within the bed induces a local oxygen depletion and, consequently, reducing microenvironments are likely to be formed.

REFERENCES

[1] J. STRINGER, *2nd. Int. Conf. on Heat-Resistant Materials*, Gatlinburg, Tennessee, 1995, pp. 19-29.
[2] J. STRINGERAND and A.J. MINCHENER, *3rd. Int. Conf. on Fluid. Bed Comb.*, London, 1984, 29, pp. 255-274.
[3] S. KUKURBAYRAK, D. BOERSMA and P. VAN DER BERG, *4th Int. Conf. on Fluid. Bed Comb.*, London, 1988, pp. 1-15.
[4] S. OKA, B. GRUBOR, B. ARSIC and D. DAKIC, *4th Int. Conf. on Fluid. Bed Comb.*, London, 1988, pp. 1-19.
[5] A.B. HART, and A.J.B. CUTLER, *Deposition and Corrosion in Gas Turbines*, John Wiley and Sons, 1973.
[6] A.J.B. CUTLER, T. FLATLEY and K.A. HAY, *Combustion* 2 (6) (1980) 17.
[7] E. RAASK, *Mineral Impurities in Coal Combustion*, Hemisphere Publish. Corp., London, 1985.
[8] E. RAASK, *The Mechanism of Corrosion by Fuel Impurities*, Butterworths Sci. Pub., London, 1963.
[9] W.T. REID, *Chemistry of Coal Utilization*, 2nd. Suppl. Vol., Wiley-Interscience, 1981, p. 1389.
[10] L.A SCANDRETT, P.h.d., Dissertation, University of Cambridge, U.K., 1983.
[11] D.R STULL and H. PROPHET, *JANAF Thermochemical Tables*, 2nd. Natl. Bureau of Standards, 1971.
[12] P.H. CRUMLEY and A.W. FLETCHER, *J. Inst. Fuel.* 29 (1956) 322.
[13] R.D. LA NAUZE, A.J. MINCHENER, E.A. ROGERS and J. STRINGER, *J. Inst. Energy.* (1979) 79-85.
[14] Y.Y. LEE, A.F. SAROFIM and J.M. BEER, *1st Int. Symp. on Fluid. Bed Comb. & Applied Techn.*, 1984, p. 85.
[15] J.F. STUBINGTON, *J. Inst. Energy.* 53 (1980) 191.
[16] A.W. NIENOW, P.N. ROWE and T. CHIBA, *AICHE Symp. Ser.* 74 (1978) 45.
[17] D. KUNII and O. LEVENSPIEL, *Fluidization Engineering*, 2nd Edition, Butterworth-Heinemann, 1991.
[18] X. ZHANG, S. WU and Y. CAO, *9th Int. Conf. on Fluid. Bed Comb.*, Boston, Mass., 1987, p. 1176.
[19] P.R. SOLOMON and M.B. COLKET, *17th Symp. (Int.) on Comb.*, The Combustion Institute, Pittsburgh, 1978, p. 131.
[20] J.P. HOLMAN, *Heat Transfer*, McGraw Hill Publish. Comp., 1990.
[21] J. LINDSAY, P.h.d., Dissertation, Cambridge University, U.K., 1983.
[22] O.A. HOUGEN, K.M. WATSON and R.A. RAGATZ, *Chemical Process Principles*, John Wiley and Sons, 1976.
[23] S. EHRLICH, *3rd. Int. Conf. on Fluid. Bed Comb.*, London, 1984, 1/1 p. 29.